IRIS AperTO

UNIVERSITÀ DEGLI STUDI DI TORINO

AperTO - Archivio Istituzionale Open Access dell'Università di Torino

Structure-Activity Relationship Studies on Tetrahydroisoquinoline Derivatives: [4′-(6,7-Dimethoxy-3,4-dihydro-1H-isoquinolin-2-ylmethyl)biphenyl-4-ol] (MC70) Conjugated through Flexible Alkyl Chains with Furazan Moieties Gives Rise to Potent and Selective Ligands of P-

This is the author's manuscript

Original Citation:

Availability:

This version is available http://hdl.handle.net/2318/1600244 since 2016-10-11T10:02:12Z

Published version:

DOI:10.1021/acs.jmedchem.6b00252

Terms of use:

Open Access

Anyone can freely access the full text of works made available as "Open Access". Works made available under a Creative Commons license can be used according to the terms and conditions of said license. Use of all other works requires consent of the right holder (author or publisher) if not exempted from copyright protection by the applicable law.

(Article begins on next page)

25 April 2024

IRIS AperTO

UNIVERSITÀ DEGLI STUDI DI TORINO

This is the author's final version of the contribution published as:

Guglielmo, Stefano; Lazzarato, Loretta; Contino, Marialessandra; Perrone, Maria G.; Chegaev, Konstantin; Carrieri, Antonio; Fruttero, Roberta; Colabufo, Nicola A.; Gasco, Alberto. Structure-Activity Relationship Studies on Tetrahydroisoquinoline Derivatives: [4′-(6,7-Dimethoxy-3,4-dihydro-1H-isoquinolin-2-ylmethyl)biphenyl-4-ol] (MC70) Conjugated through Flexible Alkyl Chains with Furazan Moieties Gives Rise to Potent and Sele.... JOURNAL OF MEDICINAL CHEMISTRY. 59 (14) pp: 6729-6738.
DOI: 10.1021/acs.jmedchem.6b00252

The publisher's version is available at:
http://pubs.acs.org/doi/pdf/10.1021/acs.jmedchem.6b00252

When citing, please refer to the published version.

Link to this full text:
http://hdl.handle.net/

This full text was downloaded from iris - AperTO: https://iris.unito.it/

iris - AperTO

University of Turin's Institutional Research Information System and Open Access Institutional Repository

SAR Studies on Tetrahydroisoquinoline Derivatives: [4'-(6,7-dimethoxy-3,4-dihydro-1H-isoquinolin-2-ylmethyl)biphenyl-4-ol] (MC70[1]) Conjugated Through Flexible Alkyl Chains with Furazan Moieties Gives Rise to Potent and Selective Ligands of P-glycoprotein.

Stefano Guglielmo,[†] Loretta Lazzarato,[†] Marialessandra Contino,[‡] Maria G. Perrone,[‡] Konstantin Chegaev,[†] Antonio Carrieri,[‡] Roberta Fruttero,[†] Nicola A. Colabufo,*[‡,§] and Alberto Gasco[†]*

[†]Dipartimento di Scienza e Tecnologia del Farmaco, Università degli Studi di Torino Via P. Giuria 9, 10125 Torino, Italy.

[‡]Dipartimento di Farmacia-Scienze del Farmaco Università degli Studi di Bari "A. Moro", Via Orabona 4, 70125, Bari (Italy)

[§]Biofordrug s.r.l., Spin-off dell'Università degli Studi di Bari "A. Moro" Via Orabona 4, 70125, Bari (Italy). Fax: (+39) 0805442231.

ABSTRACT P-glycoprotein (P-gp) is a well-known membrane transporter expressed in a number of strategic biological barriers, where it exerts a protective effect of paramount importance. Conversely it is one of the main causes of multi drug resistance (MDR), being capable of effluxing many chemotherapeutics. In a development of a previous research, a small library of compounds was created conjugating diversely substituted furazan rings with **MC70**, a well-known P-gp inhibitor. These compounds were assessed for their potency against P-gp and another transporter (MRP1), for their apparent permeability (P_{app}), and for their ability to induce ATP-ase activity, thus delineating a complete functional profile. They displayed a substrate mechanism of action and high selectivity towards P-gp, unlike the lead compound. Data relating to their activity range from low micromolar to sub-nanomolar EC_{50}, the most interesting compounds being **15** (0.97 nM), **19** (1.3 nM), **25** (0.60 nM) and **27** (0.90 nM).

Introduction

Multidrug resistance (MDR) is the major cause of the failure of cancer therapy since this phenomenon generates cancer cells that are unresponsive to chemotherapeutic agents. The most widely studied mechanism of MDR is the increased efflux of antineoplastic drugs from cells due to the overexpression of some transporters belonging to the superfamily of ATP binding cassette (ABC) transporters.[2] These proteins are ATPases, which use the energy derived from ATP hydrolysis to efflux xenobiotics. Among these transporters, P-glycoprotein (P-gp), Breast Cancer Resistance Protein (BCRP) and MultiDrug Resistance-associated Protein 1 (MRP1) are those

most frequently involved in MDR. Owing to their localization at the membranes of endothelial cells constituting barriers, such as the Blood-Brain Barrier, the Blood-Cerebrospinal fluid Barrier, and the Blood-Testis Barrier, they modulate the absorption and excretion of xenobiotics across these barriers.[3]

To overcome MDR, the co-administration of antineoplastic agents with third generation P-gp inhibitors, such as elacridar or tariquidar, has been tested, but this strategy failed in clinical trials because of pharmacokinetic and pharmacodynamic limitations: these molecules inhibited the enzyme responsible for chemotherapeutic detoxification (CYP3A4) and showed poor P-gp selectivity due to their activity towards other ABC transporters.[4-7] In addition the P-gp inhibiting mechanism of these compounds requires further clarification.

NO-donors, i.e. pro-drugs of nitric oxide (NO), a well-known and ubiquitous endogenous messenger in the human body, have also been reported to reduce the efflux of doxorubicin (DOXO) from HT29-dx cancer cells, following nitration of tyrosine residues of some transporters, including P-gp.[8,9] Based on these assumptions, another strategy proposed to overcome MDR is the administration of dual drugs, in which an anticancer agent is linked to an appropriate NO-donor moiety.[10,11]

Owing to its strategic localization at the Blood-Brain Barrier, P-gp also represents a crucial defense mechanism for the central nervous system: changes in P-gp expression and function are believed to occur in the early stages of several neurological disorders, such as epilepsy, Alzheimer's disease (AD) and Parkinson's disease (PD).[12a,b] Taken together, these considerations might make the transporter a valuable target for noninvasive imaging techniques, such as

Positron Emission Tomography (PET) and Single-Photon Computed Emission Tomography (SPECT), used for early diagnosis of such disorders.

Biphenyl derivatives bearing a tetrahydroisoquinoline moiety have emerged as an important class of products displaying P-gp inhibiting activity, and among these one of the most interesting is compound **1** (**MC70**[1]) (Chart 1). It is endowed with strong inhibitory potency (EC_{50} = 0.69 μM) but with poor P-gp selectivity.[1]

Chart 1. Structure of **MC70** (**1**).

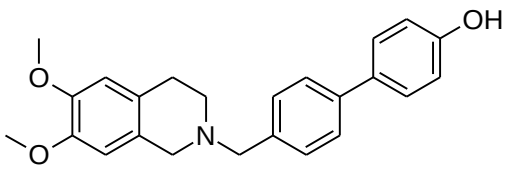

Recent results obtained by the authors show that the insertion between the biphenyl fragment and the basic tetrahydroisoquinoline ring of a flexible alkyl chain of variable length gives rise to potent and selective P-gp ligands.[13] Another study found that the direct linking of flexible alkyl chains to the phenolic group of **1** affords agents endowed with high activity and selectivity towards P-gp. In particular, when the alkyl chain is an *n*-butyl group, the resulting activity falls in the nM range (EC_{50} = 5.2 nM).[14] Other results in authors' hands indicate that some furazans (1,2,5-oxadiazoles) display activity towards P-gp.[9,15]

On the basis of these findings, a series of compounds was designed in which the phenolic group of the biphenyl moiety of **1** is joined, through an alkyl bridge of variable length, to a number of furazan derivatives bearing substituents endowed with different stereoelectronic and lipophilic properties. This paper reports the synthesis of this small library of products; it shows that all of them are selective P-gp transporter modulator, and that some of them display activity in

nanomolar and sub-nanomolar range, thus making them interesting leads for the development of cancer chemotherapy co-adjuvants and potential radiotracers to image P-gp activity in vivo through PET.

Results and discussion.

Chemistry. All target compounds were synthesized in a straightforward manner, by coupling the appropriate derivative of **1** (**2**, **21**, **29**) with phenylsulfonylfurazan derivatives (Scheme 1). Some of the latter intermediates were obtained with reported procedures (see experimental section). Conversely, furazans **6**, **7** and **9** were obtained by alcoholysis of 3,4-bis(phenylsulfonyl)furazan with 1,8-diazabicyclo[5.4.0]undec-7-ene (DBU) as base in CH_2Cl_2. Furazan **10** was synthesized by refluxing the parent furoxan **31** in trimethylphosphite (Scheme 2).

As for the hydroxyalkyl derivatives of **1**, **2** has already been reported in the literature (see experimental section), whilst **21** was obtained by heating **1** to 110 °C with ethylene carbonate and K_2CO_3 in DMF, and **29** was synthesized by alkylating **1** with 4-chlorobutan-1-ol in CH_3CN with Cs_2CO_3 as base (Scheme 1).

The hydroxyalkyl derivatives were then functionalized with the furazan moieties, by reaction with the appropriate phenysulfonylfurazan intermediates, using NaH in THF, thus affording the target compounds in 25 to 80% yields (see experimental section). Compounds bearing the phenylsulfinyl substituent (**19** and **27**) were obtained by oxidizing the parent sulfides with H_2O_2 in acidic environment, in order to minimize oxidation of tetrahydroisoquinoline nitrogen atom.

The two cyano derivatives (**20** and **28**) were synthesized by dehydration of the corresponding amides **18** and **26**, using trifluoroacetic anhydride (TFAA) and Et_3N in THF.

Scheme 1. Synthesis of target compounds.[a]

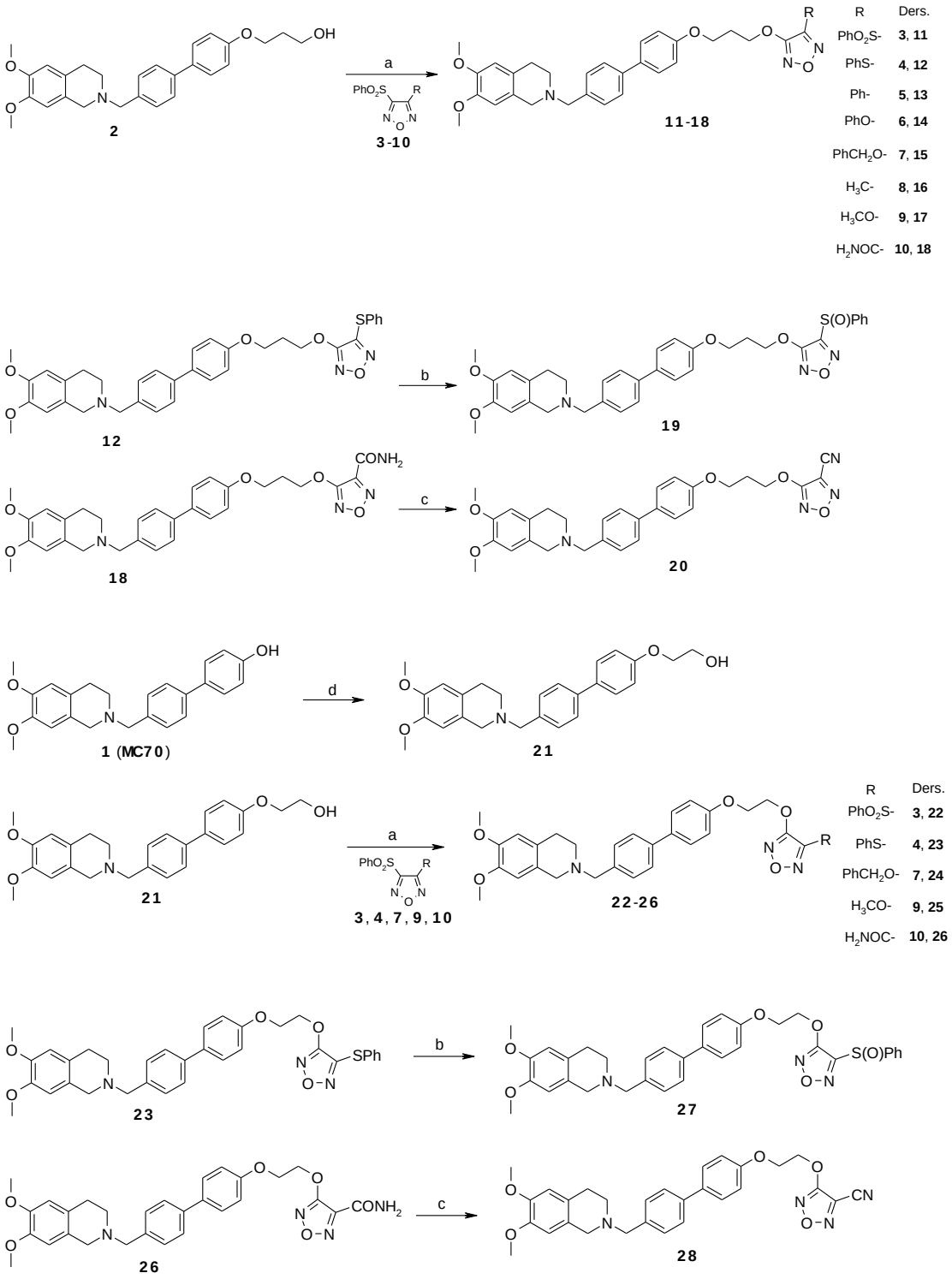

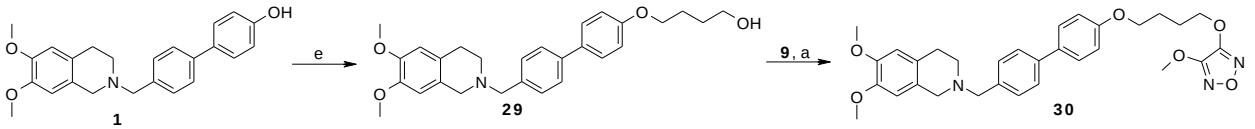

[a]Reagents and conditions: a) NaH 60% mineral oil suspension, THF, reflux. b) H_2O_2 30%, TFA, 0 °C. c) TFAA, Et_3N, THF. d) Ethylene carbonate, K_2CO_3, DMF, 110 °C. e) 4-chlorobutan-1-ol, Cs_2CO_3, KI cat., CH_3CN, 70 °C.

Scheme 2. Synthesis of the furazan intermediates.[a]

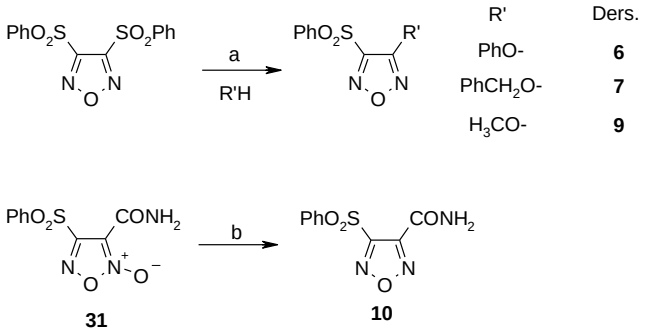

[a]Reagents and conditions: a) DBU, CH_2Cl_2, room temp. b) $(CH_3O)_3P$, reflux.

Biology

All compounds were tested in order to determine their P-gp potency, selectivity, and the interacting mechanisms, by three assays[13]: 1) inhibition of transport of the profluorescent P-gp substrate Calcein-AM; 2) determination of the cellular ATP level; 3) determination of the apparent permeability (P_{app}). These assays define the potency of the interaction towards P-gp (calcein AM assay on MDCK cells overexpressing P-gp), the selectivity of the ligands, by establishing the activity towards MRP1 (calcein AM on MDCK assay overexpressing MRP1) and the activity profile (substrate and inhibitor) by a combination of the above three assays. Moreover for the most potent compounds (**19**, **27**, **25** and **15**) the biological characterization was

extended to BCRP inhibition assay and toxicity assay on two cell lines: MDCK-MDR1 and wt-MCF7.

In general, since they are transported, substrates inhibit the transport of Calcein-AM, induce a decrease in ATP cell level, and have P_{app} value > 2. By contrast, inhibitors are not transported, they inhibit the transport of Calcein-AM, do not induce a decrease in ATP level, and have P_{app} value < 2. The results of these assays are reported in Table 1. Analysis of the data show that all of the compounds reported in the present study, displaying P_{app} > 2, can be classified as P-gp substrates, but that they are unable to induce ATPase activity; the ATPase activity observed for compound **25** may be due to the poor hindrance of side chain and furazan moiety, which could be expected to afford a more "efficient" interaction with the target, and thus to activate ATPase, albeit weakly.

Table 1 clearly shows that the P-gp activity (EC_{50}) of these products is closely dependent on the nature of the substituents at the ring and on the length of the flexible chain linking the furazan system to **1**. Despite this ample range of potency towards P-gp, all compounds are inactive against MRP1, thus showing themselves to be selective ligands. As for **19**, **27**, **25** and **15**, being the most potent members of the series, they were further studied to asses selectivity and toxicity. They proved inactive towards BCRP transporter (EC_{50} > 100 μM). They were not toxic towards MDCK-MDR1 after 24 hours at 1 μM concentration, while showed toxicity after 48 hours at 0.1 μM concentration; as for wt-MCF7 cells, the test compounds displayed toxicity after 24 hours at 0.1 μM concentration (data non shown). These results further confirmed the selectivity of the most potent ligands and showed the presence of toxicity only for concentration values considerably higher than the biologically effective ones.

Table 1. Biological activity profile of target compounds.

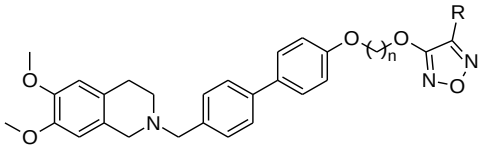

			EC_{50} ± SEM (nM)[a]			
compound	**n**	**R**	**MDR1**	**MRP1**	**P_{app}[c]**	**ATPase activation**
13	3	Ph-	3300 ± 600	NA[b]	20	No
14	3	PhO-	1180 ± 220	NA	3.8	No
12	3	PhS-	1170 ± 230	NA	4.7	No
19	3	PhSO-	1.3 ± 0.3	NA	2.6	No
27	2	PhSO-	0.90 ± 0.2	NA	4.6	No
11	3	$PhSO_2$-	380 ± 70	NA	2.5	No
16	3	CH_3-	350 ± 50	NA	4.0	No
17	3	CH_3O-	54 ± 10	NA	3.2	No
25	2	CH_3O-	0.60 ± 0.10	NA	3.2	Yes
30	4	CH_3O-	290 ± 53	NA	3.0	No
15	3	$PhCH_2O$-	0.97 ± 0.20	NA	3.0	No
24	2	$PhCH_2O$-	290 ± 50	NA	4.9	No
20	3	-CN	1050 ± 100	NA	4.9	No
28	2	-CN	1200 ± 90	NA	4.7	No

[a]The value is the mean of three independent experiments, sample in duplicate; [b]not active at 10^{-4} M; [c]apparent permeability (the value is from two independent experiments).

Owing to the limited extension of the library, and the structural complexity of the biological target, a clear relationship between the structure of the products and their activity does not emerge from this puzzling picture. However a molecular modeling study has highlighted the role of some key interactions with the target, ascribable to hydrogen bonds and steric and hydrophobic interactions. This study was done by applying docking and homology modeling techniques to selected compounds (**15**, **17**, **25** and **30**), exploiting a model of human P-gp created *in-house*, using a comparative approach based on recent crystallographic data for mouse P-gp (pdbcode 4Q9H).[16,17] Unlike the first P-gp structure, crystallized by Aller et al.[18], the latest data reported by Szewczyk show a P-gp molecular skeleton with a wider cleft, into which hydrophobic drugs and lipids might more easily fit. However some structural traits are conserved: there are two symmetrical halves comprising six helices, as well as two ATP binding clefts. This structure would afford ligand entry via the "inward facing" elbow helix binding site, with a large internal cavity open towards the cytoplasm and the inner edge of the lipid bilayer. Having this "inward facing" binding site, substrates are almost "pulled out" of the cell as soon as they pass the layer, with an "outward facing" flip of the P-gp scaffold. This study aimed to prove this hypothesis, by challenging the P-gp flipping depending on the molecular shape and pharmacophoric elements of the inhibitors presented herein.

Having assembled the scaffold of human P-gp, the conformational space was sampled for the most active compound, **25**, with a molecular dynamics simulation carried out in octanol as solvation milieu, so as to reproduce the type of environment of the drug transport to the inner cell process more closely. Given the greatly extended protein surface, and the potential multiple anchoring points differentiating substrates and inhibitors, the following protocol was applied: the entire database, comprising two thousand conformers of **25**, was initially screened using VINA,

after which the binding mode was refined with a more accurate docking method using AUTODOCK.[19]

As may be seen from Figure 1, during binding to P-gp, **25** achieves extensive favorable contacts and π–π stackings, with diverse residues located at the large cervix of the two transmembrane domains: the tetrahydroisoquinoline ring occupies the mainly hydrophobic receptor slot, surrounded by Tyr310, Tyr307 and Gln725. Tyr310 links the protonated nitrogen via a charge-reinforced hydrogen bond, whereas the latter two residues engage polar contacts with the methoxy group of the ligand. Moreover, the para substituted diphenyl pendant redirects the alkyl chain bearing the furazan ring towards a more occluded and less hydrophobic lodging, where the phenoxy oxygen anchors the ligand to the side chain of Gln347, while the furazan ring and the methoxy group stabilize the receptor-ligand complex, forming a significant hydrogen bond with the amide nitrogen of Gln195. The free energy of binding relative to **25** is -6.38 kcal/mol, and it is worth noting that the elongation of the alkyl chain considerably hampers attainment of this binding pose: the less potent compounds, **17** and **30**, bearing a longer spacer, are not capable of correctly recruiting all the favorable interactions of **25**, and thereafter bind to P-gp with less favorable energies (-5.91 and -5.35 kcal/mol, respectively). The low activity of product **14** may be the consequence of the unfavorable length of the spacer combined with the steric bulk of the phenyl ring. As for products **13**, **12**, **16**, **20** and **28**, the presence at the furazan ring of substituents unable to give the interaction reported above significantly decreases their activity. Finally, compound **15**, though having the same spacer as **17**, recruits additional hydrophobic interactions, since its benzyloxy substituent is able to establish a significant π–π stacking with the aromatic ring of Tyr950, as proved by the better binding energy (-6.23 kcal/mol). Derivative **24** presumably cannot be able to engage in this additional interaction owing to the shorter alkyl

spacer. As a figure of merit, for compounds **17**, **25**, **30** and **15**, the experimental pEC_{50} data are correctly ranked by the free energy of docking being the correlation coefficient $r^2 > 0.9$.

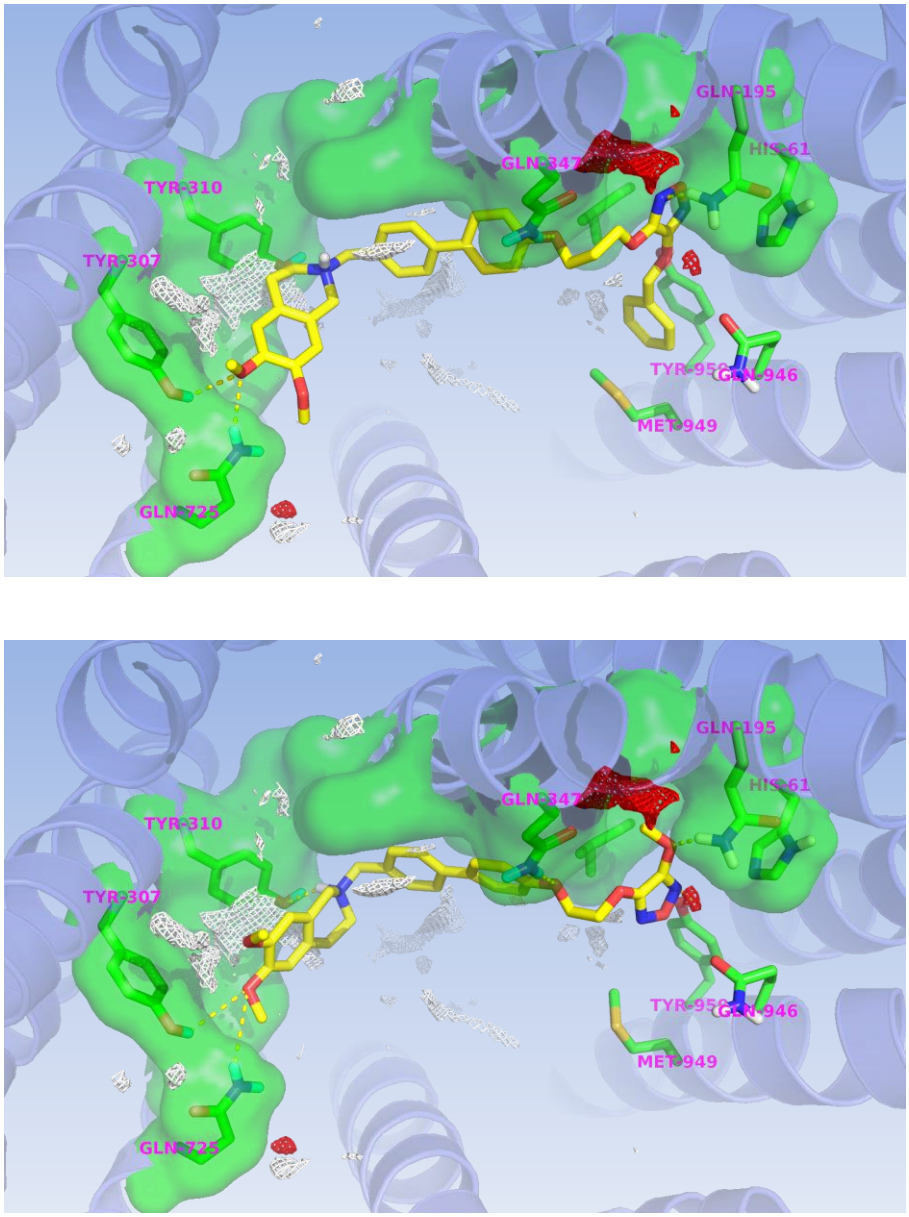

Figure 1. Intracellular view of the docking pose for **15** (top) and **25** (bottom) to the P-gp binding site. The GRID[20] molecular interaction fields (white hydrophobic (DRY), red hydrogen bond accepting (O) probes) are contoured at -1.5 and -6.5 kcal/mol, respectively; to facilitate

interpretations, side chains of residues generating favorable interactions with the receptor are displayed.

The very high activity of compounds **19** and **27** is not explained through the present model and thus these two derivatives deserve further investigation. The partial loss of activity observed for **11** (the sulfone analog of **19**) could be due to the increased electrophilic reactivity of sulfonylfurazan moiety, which possibly undergoes nucleophilic attack before reaching the binding site.

Conclusion

The present study extends the modulation of **1** that was begun in a previous research, synthesizing a small library of compounds in which **1** is formally linked through an alkyl spacer to diversely-substituted furazan rings. The potency of the compounds is widely distributed, with EC_{50} values ranging from the sub-nanomolar to the low micromolar. A common feature emerged: functionalization of the phenolic group of the lead compound modifies the functional profile, **1** being a poorly selective inhibitor, while all the compounds obtained in this study act as substrates with medium to very high affinity and are highly selective towards P-gp.

The nanomolar activity, the high selectivity and the absence of toxicity characterizing some members of the series (**19**, **27**, **25** and **15**) make them potential candidates for reverting MDR, by co-administration of chemotherapeutic drugs and P-gp modulating agents. Moreover, their high affinity substrate profile is attractive in view of their possible employment in *in vivo* imaging of the function of P-gp through non-invasive imaging techniques such as PET and SPECT. The finding that the furazan ring is a useful and versatile decoration to conjugate with the structure of

1 opens interesting perspectives for the synthesis of new, potent, and selective P-gp ligands through appropriate modulation of the substituent on the heterocyclic ring.

Experimental Section

Chemistry. Materials and instrumentation. ^{1}H and ^{13}C-NMR spectra were recorded on a Bruker Avance 300 at 300 and 75 MHz respectively, using $SiMe_4$ as internal reference. Chemical shifts (δ) are given in parts per million (ppm) and the coupling constants (J) in Hertz (Hz). The following abbreviations are used to designate the multiplicities: s = singlet, d = doublet, t = triplet, q = quartet, quin = quintet, sxt = sextet, m = multiplet. Low resolution mass spectra were recorded on a Finnigan-Mat TSQ-700 with chemical ionization or on a Micromass Quattro micro^{TM} API (Waters Corporation, Milford, MA, USA) with electrospray ionization. Melting points (mp) were determined with a capillary apparatus (Büchi 540). Flash column chromatography was performed on silica gel (Merck Kieselgel 60, 230-400 mesh ASTM). The progress of the reactions was followed by thin layer chromatography (TLC) on 5×20 cm plates with a layer thickness of 0.2 mm. The purity of all target compounds was assessed by RP-HPLC and was > 95%. Analyses were performed on a HP1100 chromatograph system (Agilent Technologies, Palo Alto, CA, USA). The analytical column was a LiChrosphere® C18 5µM (Merck KGaA, 64271 Darmstadt, Germany). UV signals were recorded at 210, 226 and 254 nm. All compounds were dissolved in eluent and injected through a 20 µL loop.

Compounds **1**,[14] **2**,[14] **3**,[21] **4**,[22] **5**,[23] **8**[24] and **31**[9] were prepared following reported procedures.

General procedure for the synthesis of compounds 11 – 18, 22 – 26 and 30. Derivative **2** (for **11** – **18**), **21** (for **22** – **26**) or **29** (for **30**) were mixed with the appropriate phenylsulfonylfurazan derivative (1 eq.) and NaH 60 % suspension in mineral oil (2 eq) in anhydrous THF. The mixture

was stirred at reflux overnight, then it was diluted with water and extracted with CH_2Cl_2. The organic extracts were washed with brine, dried over Na_2SO_4, filtered and evaporated under reduced pressure. The crude was purified by means of flash chromatography on silica gel as reported.

6,7-Dimethoxy-2-((4'-(3-((4-(phenylsulfonyl)-1,2,5-oxadiazol-3-yl)oxy)propoxy)biphen-4-yl)methyl)-1,2,3,4-tetrahydroisoquinoline (11). White solid. Yield 80% (CH_2Cl_2/EtOAc 90/10). An analytical sample was obtained dissolving the product in anhydrous dioxane and dropping a 6M solution of HCl into anhydrous dioxane at 0 °C. The white solid which separated was collected and recrystallized from MeOH/Et_2O.^{1}H NMR ($CDCl_3$) δ 7.98 (d, J = 7.2 Hz, 2H), 7.67 (t, J = 7.0 Hz, 1H), 7.44-7.61 (m, 8H), 6.99 (d, J = 8.7 Hz, 2H), 6.61 (s, 1H), 6.50 (s, 1H), 4.60 (t, J = 6.0 Hz, 2H), 4.13 (t, J = 6.0 Hz, 2H), 3.86 (s, 3H), 3.84 (s, 3H), 3.71 (s, 2H), 3.58 (s, 2H), 2.74-2.84 (m, 4H), 2.33 (quin, J = 6.0 Hz, 2H). ^{13}C NMR ($CDCl_3$) δ 161.8, 159.1, 149.6, 149.1, 148.5, 141.5, 137.7, 137.0, 132.9, 132.6, 131.0, 129.5, 129.1, 128.8, 127.2, 124.2, 120.7, 115.8, 112.2, 110.6, 71.8, 64.6, 58.8, 56.40, 56.36, 51.6, 49.6, 28.8, 25.4. MS CI (*i*-butane) *m/z* 642 $[M + H]^+$; mp = 180.0-181.5 °C dec. (recrystallized from MeOH/Et_2O). Purity: ≥ 99%, t_r: 4.7 min., eluent: CH_3CN/H_2O 70/30 0.1% TFA, fl: 1.0 mL/min.

6,7-Dimethoxy-2-((4'-(3-((4-(phenylsulfenyl)-1,2,5-oxadiazol-3-yl)oxy)propoxy)biphen-4-yl)methyl)-1,2,3,4-tetrahydroisoquinoline (12). White solid. Yield 67% (CH_2Cl_2/EtOAc 90/10). ^{1}H NMR ($CDCl_3$) δ 7.52-7.55 (m, 7H), 7.45 (d, J = 8.1 Hz, 2H), 7.33-7.35 (m, 2H), 6.92 (d, J = 8.4 Hz, 2H), 6.91 (s, 1H), 6.50 (s, 1H), 4.52 (t, J = 6.0 Hz, 2H), 3.98 (t, J = 6.0 Hz, 2H), 3.84 (s, 3H), 3.81 (s, 3H), 3.71 (s, 2H), 3.58 (s, 2H), 2.84 (t, J = 5.1 Hz, 2H), 2.77 (t, J = 5.1 Hz, 2H), 2.22 (quin, 5.9 Hz, 2H). ^{13}C NMR ($CDCl_3$) δ 163.4, 158.1, 147.5, 147.1, 144.2, 139.5, 137.0, 133.8, 133.0, 129.54, 129.51, 129.3, 128.0, 127.9, 126.7, 126.6, 126.2, 114.8, 111.4,

109.4, 69.3, 63.5, 62.5, 55.9 (two overlapping peaks), 55.7, 50.8, 28.74, 28.71. MS CI (*i*-butane) *m/z* 610 $[M + H]^+$; mp = 102.5-103.2 °C (recrystallized from MeOH). Purity: 99%, t_r: 4.8 min., eluent: CH_3CN/H_2O 60/40 0.1% TFA, fl: 1.2 mL/min.

6,7-Dimethoxy-2-((4'-(3-((4-phenyl-1,2,5-oxadiazol-3-yl)oxy)propoxy)biphen-4-yl)methyl)-1,2,3,4-tetrahydroisoquinoline (13). White solid. Yield 51% (CH_2Cl_2/EtOAc 90/10). ^{1}H NMR ($CDCl_3$) δ 7.96-7.99 (m, 2H), 7.43-7.54 (m, 9H), 6.97 (d, J = 8.7 Hz, 2H), 6.61 (s, 1H), 6.50 (s, 1H), 4.70 (t, J = 6.0 Hz, 2H), 4.21 (t, J = 6.0 Hz, 2H), 3.84 (s, 3H), 3.80 (s, 3H), 3.71 (s, 2H), 3.58 (s, 2H), 2.76-2.84 (m, 4H), 2.40-2.44 (m, 2H). ^{13}C NMR ($CDCl_3$) δ 163.5, 158.1, 147.5, 147.2, 145.2, 139.5, 137.0, 133.8, 130.7, 129.5, 129.0, 128.1, 127.4, 126.8, 126.6, 126.2, 125.2, 114.8, 111.4, 109.5, 69.7, 64.1, 62.4, 55.9 (two overlapping peaks), 55.7, 50.8, 28.9, 28.8. MS CI (*i*-butane) *m/z* 578 $[M + H]^+$; mp = 119.0-119.7 °C (recrystallized from EtOH). Purity: 99%, t_r: 6.0 min., eluent: CH_3CN/H_2O 70/30 0.1% TFA, fl: 1.2 mL/min.

6,7-Dimethoxy-2-((4'-(3-((4-phenoxy-1,2,5-oxadiazol-3-yl)oxy)propoxy)biphen-4-yl)methyl)-1,2,3,4-tetrahydroisoquinoline (14). White solid. Yield 62% (CH_2Cl_2/EtOAc 90/10). ^{1}H NMR ($CDCl_3$) δ 7.53 (m, 4H), 7.37-7.46 (m, 4H), 7.30-7.32 (m, 2H), 6.97 (d, J = 8.8 Hz, 2H), 6.91 (s, 1H), 6.50 (s, 1H), 4.62 (t, J = 6.2 Hz, 2H), 4.15 (t, J = 6.0 Hz, 2H), 3.84 (s, 3H), 3.81 (s, 3H), 3.71 (s, 2H), 3.58 (s, 2H), 2.84 (t, J= 5.1 Hz, 2H), 2.76 (t, J= 5.1 Hz, 2H), 2.35 (quin, J = 5.9 Hz, 2H). ^{13}C NMR ($CDCl_3$) δ 158.1, 157.0, 155.3, 154.1, 147.5, 147.1, 139.5, 136.9, 134.5, 133.8, 129.8, 129.5, 128.1, 126.7, 126.6, 126.2, 125.8, 118.8, 114.8, 111.4, 109.4, 69.4, 63.6, 55.9 (two overlapping peaks), 55.7, 50.8, 28.8, 28.7. MS CI (*i*-butane) *m/z* 594 $[M + H]^+$; mp = 91.6-92.3 °C (recrystallized from *i*PrOH). Purity: 99%, t_r: 5.9 min., eluent: CH_3CN/H_2O 70/30 0.1% TFA, fl: 1 mL/min.

6,7-Dimethoxy-2-((4'-(3-((4-benzyloxy-1,2,5-oxadiazol-3-yl)oxy)propoxy)biphen-4-yl)methyl)-1,2,3,4-tetrahydroisoquinoline (15). White solid. Yield 57% (CH_2Cl_2/EtOAc 90/10). ^{1}H NMR ($CDCl_3$) δ 7.51 (m, 4H), 7.44 (m, 5H), 7.38 (m, 2H), 6.94 (d, J = 8.8 Hz, 2H), 6.60 (s, 1H), 6.49 (s, 1H), 5.32 (s, 2H), 4.54 (t, J = 6.0 Hz, 2H), 4.13 (t, J = 5.9 Hz, 2H), 3.83 (s, 3H), 3.80 (s, 3H), 3.72 (s, 2H), 3.59 (s, 2H), 2.84 (t, J = 5.1 Hz, 2H), 2.77 (t, J = 5.1 Hz, 2H), 2.31 (quin, J = 5.9 Hz, 2H). ^{13}C NMR ($CDCl_3$) δ 158.1, 156.4, 156.2, 147.5, 147.2, 139.6, 136.6, 134.4, 133.6, 129.6, 129.0, 128.8, 128.7, 128.0, 126.6, 126.4, 126.1, 114.7, 111.3, 109.4, 74.0, 69.2, 63.7, 62.3, 55.86, 55.85, 55.5, 50.7, 28.7, 28.6. MS CI (*i*-butane) *m/z* 608 $[M + H]^+$, mp = 94.5-95.3 °C (recrystallized from MeOH). Purity: 99%, t_r: 6.0 min., eluent: CH_3CN/H_2O 70/30 0.1% TFA, fl: 1.2 mL/min.

6,7-Dimethoxy-2-((4'-(3-((4-methyl-1,2,5-oxadiazol-3-yl)oxy)propoxy)biphen-4-yl)methyl)-1,2,3,4-tetrahydroisoquinoline (16). White solid. Yield 68% (CH_2Cl_2/EtOAc 90/10). ^{1}H NMR ($CDCl_3$) δ 7.53 (m, 4H), 7.44 (d, J = 8.0 Hz, 2H), 6.97 (d, J = 8.8 Hz, 2H), 6.61 (s, 1H), 6.50 (s, 1H), 4.56 (t, J = 6.2 Hz, 2H), 4.17 (t, J = 5.9 Hz, 2H), 3.84 (s, 3H), 3.81 (s, 3H), 3.71 (s, 2H), 3.58 (s, 2H), 2.84 (t, J = 5.2 Hz, 2H), 2.76 (t, J = 5.2 Hz, 2H), 2.34 (quin, J = 6.0 Hz, 2H), 2.27 (s, 3H). ^{13}C NMR ($CDCl_3$) δ 164.4, 158.1, 147.5, 147.2, 139.5, 137.0, 133.8, 131.6, 129.5, 128.1, 126.8, 126.6, 126.2, 114.7, 111.4, 109.5, 69.0, 63.8, 62.5, 55.9 (two overlapping peaks), 55.7, 50.8, 28.82, 28.76, 7.27. MS CI (*i*-butane) *m/z* 516 $[M + H]^+$; mp = 93.0-93.9 °C (recrystallized from EtOH). Purity: 99%, t_r: 5.5 min., eluent: CH_3CN/H_2O 60/40 0.1% TFA, fl: 1.2 mL/min.

6,7-Dimethoxy-2-((4'-(3-((4-methoxy-1,2,5-oxadiazol-3-yl)oxy)propoxy)biphen-4-yl)methyl)-1,2,3,4-tetrahydroisoquinoline (17). White solid. Yield 73% (CH_2Cl_2/EtOAc 90/10). ^{1}H NMR ($CDCl_3$) δ 7.53 (m, 4H), 7.44 (d, J = 8.1 Hz, 2H), 6.97 (d, J = 8.8 Hz, 2H), 6.61 (s, 1H), 6.50 (s, 1H), 4.57, (t, J = 6.2 Hz, 2H), 4.17 (t, J = 6.0 Hz, 2H), 4.09 (s, 3H), 3.84 (s, 3H),

3.81 (s, 3H), 3.71 (s, 2H), 3.58 (s, 2H), 2.84 (t, J = 5.1 Hz, 2H), 2.76 (t, J = 5.1 Hz, 2H), 2.34 (quin, J = 6.0 Hz, 2H).^{13}C NMR ($CDCl_3$) δ 158.1, 157.0, 156.3, 147.5, 147.2, 139.6, 136.9, 133.8, 129.5, 128.1, 126.7, 126.6, 126.2, 114.8, 111.4, 109.5, 69.2, 63.7, 62.4, 59.2, 55.9, 55.7, 50.8, 30.9, 28.8, 28.7. MS CI (*i*-butane) *m/z* 532 $[M + H]^+$; mp = 100.3-101.1 °C (recrystallized from *i*PrOH). Purity: 99%, t_r: 7.2 min., eluent: CH_3CN/H_2O 55/45 0.1% TFA, fl: 1.2 mL/min.

4-(3-((4'-((6,7-Dimethoxy-3,4-dihydroisoquinolin-2(1*H*)-yl)methyl)biphenyl-4-yl)oxy)propoxy)-1,2,5-oxadiazol-3-carboxyamide (18). White solid. Yield 42% (CH_2Cl_2/EtOAc 50/50). ^{1}H NMR ($CDCl_3$) δ 7.52 (m, 4H), 7.43 (d, J = 8.2 Hz, 2H), 6.96 (d, J = 8.8 Hz, 2H), 6.68 (br s, 1H), 6.60 (s, 1H), 6.49 (s, 1H), 6.19 (br s, 1H), 4.67 (t, J = 6.0 Hz, 2H), 4.19 (t, J = 5.8 Hz, 2H), 3.84 (s, 3H), 3.81 (s, 3H), 3.71 (s, 2H), 3.58 (s, 2H), 2.84 (t, J = 5.0 Hz, 2H), 2.77 (t, J= 5.5 Hz, 2H), 2.40 (quin, J = 5.9 Hz, 2H). ^{13}C NMR ($CDCl_3$) δ 163.5, 158.0, 157.3, 154.3, 147.5, 147.2, 139.5, 136.9, 133.8, 129.6, 128.1, 126.64, 126.58, 126.17, 114.7, 111.4, 109.5, 70.5, 63.9, 62.4, 55.90, 55.88, 55.7, 50.8, 28.74, 28.68. MS ESI+ *m/z* 545 $[M + H]^+$; mp = 160.3-161.0 °C (recrystallized from $MeOH/H_2O$).

6,7-Dimethoxy-2-((4'-(3-((4-(phenylsulfinyl)-1,2,5-oxadiazol-3-yl)oxy)propoxy)biphen-4-yl)methyl)-1,2,3,4-tetrahydroisoquinoline (19). Yield 74% (petroleum ether/acetone 80/20). The reaction was carried out following a reported procedure.[25] ^{1}H NMR ($CDCl_3$) δ 7.73 (m, 2H), 7.55 (m, 4H), 7.47 (m, 5H), 6.91 (d, J = 8.8 Hz, 2H), 6.61 (s, 1H), 6.50 (s, 1H), 4.48 (m, 2H), 3.93 (m, 2H), 3.84 (s, 3H), 3.80 (s, 3H), 3.72 (s, 2H), 3.59 (s, 2H), 2.85 (t, J = 5.1 Hz, 2H), 2.77 (t, J = 5.1 Hz, 2H), 2.19 (quin, J= 5.9 Hz, 2H). ^{13}C NMR ($CDCl_3$) δ 162.2, 158.0, 151.0, 147.4, 147.1, 139.49, 139.47, 136.8, 133.8, 132.3, 129.6, 129.5, 128.0, 126.6, 126.5, 126.1, 124.8, 114.7, 111.4, 109.4, 69.9, 63.3, 62.3, 55.9 (two overlapping peaks), 55.6, 50.8, 28.6, 28.5. MS

ESI+ *m/z* 626 $[M + H]^+$. Purity: 99%, t_r: 6.7 min., eluent: CH_3CN/H_2O 60/40 0.1% TFA, fl: 1.2 mL/min.

4-(3-((4'-((6,7-Dimethoxy-3,4-dihydroisoquinolin-2(1*H*)-yl)methyl)biphenyl-4-yl)oxy)propoxy)-1,2,5-oxadiazol-3-carbonitrile (20). Compound **18** was solubilized in THF. The solution was cooled in an ice bath and Et_3N (4 eq) and TFAA (4 eq). were added. The mixture was stirred at room temperature overnight, after which the solvent was removed under reduced pressure, the residue was taken up with CH_2Cl_2 and washed with 0.5 N NaOH, water (3 times) and brine. The organic layer was dried over Na_2SO_4, filtered and evaporated under reduced pressure. The crude product was purified through flash chromatography on silica gel, eluting with petroleum ether/EtOAc 60/40 to afford the title product as a white sticky solid in 60% yield. ^{1}H NMR ($CDCl_3$) δ 7.54 (m, 4H), 7.47 (m, 2H), 6.97, (d, J = 8.8 Hz, 2H), 6.61 (s, 1H), 6.49 (s, 1H), 4.68 (t, J = 6.0 Hz, 2H), 4.19 (t, J = 5.8 Hz, 2H), 3.84 (s, 3H), 3.81 (s, 3H), 3.77 (s, 2H), 3.64 (s, 2H), 2.86 (m, 4H), 2.38 (quin, J = 6.0 Hz, 2H). ^{13}C NMR ($CDCl_3$) δ 165.3, 164.7, 158.0, 156.8, 147.6, 147.3, 133.9, 131.4, 129.8, 128.2, 126.7, 125.8, 125.6, 114.7, 111.4, 109.4, 106.3, 71.0, 63.3, 62.4, 55.91, 55.88, 55.7, 50.6, 28.6 (two overlapping peaks). MS ESI+ *m/z* 527 $[M + H]^+$. Purity: 98%, t_r: 6.2 min., eluent: CH_3CN/H_2O 60/40 0.1% TFA, fl: 1.2 mL/min.

2-((4'-((6,7-Dimethoxy-3,4-dihydroisoquinolin-2(1*H*)-yl)methyl)biphenyl-4-yl)oxy)ethan-1-ol (21). Ethylene carbonate (2 eq) and K_2CO_3 (1 eq) were added to a solution of **1** in DMF. The mixture was stirred at 110 °C for 6 hours, then diluted with water and extracted with CH_2Cl_2 (3 times). The organic extracts were washed with water (3 times) and brine, dried over Na_2SO_4, filtered and evaporated under reduced pressure. The crude product was purified through flash chromatography on silica gel eluting with petroleum ether/acetone 70/30, affording the title

product as a white solid in 72% yield. ^{1}H NMR ($CDCl_3$) δ 7.53 (m, 4H), 7.44 (d, J = 8.1 Hz, 2H), 6.98 (d, J = 8.8 Hz, 2H), 6.60 (s, 1H), 6.49 (s, 1H), 4.11 (t, J = 4.5 Hz, 2H), 3.96 (t, J = 4.2 Hz, 2H), 3.84 (s, 3H), 3.80 (s, 3H), 3.71 (s, 2H), 3.58 (s, 2H), 2.84 (t, J = 5.1 Hz, 2H), 2.71 (t, J = 5.1 Hz, 2H).^{13}C NMR ($CDCl_3$) δ 158.1, 147.5, 147.2, 139.5, 136.8, 133.9, 129.6, 128.09, 126.62, 126.58, 126.2, 114.8, 111.4, 109.4, 69.3, 62.4, 61.4, 55.90, 55.88, 55.7, 50.8, 28.7. MS CI (*i*-butane) *m/z* 420 $[M + H]^+$; mp = 130.6-131.1 °C (recrystallized from MeOH).

6,7-Dimethoxy-2-((4'-(3-((4-(phenylsulfonyl)-1,2,5-oxadiazol-3-yl)oxy)ethoxy)biphen-4-yl)methyl)-1,2,3,4-tetrahydroisoquinoline (22). Sticky solid. Yield 85% (CH_2Cl_2/EtOAc 90/10). ^{1}H NMR ($CDCl_3$) δ 8.08 (d, J = 8.0 Hz, 2H), 7.67 (m, 1H), 7.52 (m, 8H), 6.97 (d, J = 8.8 Hz, 2H), 6.61 (s, 1H), 6.50 (s, 1H), 4.72 (t, J= 4.2 Hz, 2H), 4.37 (t, J= 4.2 Hz, 2H), 3.84 (s, 3H), 3.81 (s, 3H), 3.72 (s, 2H), 3.59 (s, 2H), 2.85 (t, J = 4.9 Hz, 2H), 2.77 (t, J = 4.9 Hz, 2H). ^{13}C NMR ($CDCl_3$) δ 161.2, 157.6, 148.8, 147.4, 147.1, 139.3, 137.6, 137.2, 135.4, 134.4, 129.60, 129.57, 129.0, 128.2, 126.7, 126.6, 126.2, 114.8, 111.4, 109.4, 71.8, 65.4, 62.4, 55.9 (two overlapping peaks), 55.7, 50.8, 28.7. MS CI (*i*-butane) *m/z* 628 $[M + H]^+$.

6,7-Dimethoxy-2-((4'-(3-((4-benzyloxy-1,2,5-oxadiazol-3-yl)oxy)ethoxy)biphen-4-yl)methyl)-1,2,3,4-tetrahydroisoquinoline (24). White solid. Yield 72% (CH_2Cl_2/EtOAc 80/20). ^{1}H NMR ($CDCl_3$) δ 7.55 (m, 4H), 7.46 (m, 5H), 7.37 (m, 2H), 6.98 (d, J = 8.5 Hz, 2H), 6.61 (s, 1H), 6.49 (s, 1H), 5.34 (s, 2H), 4.70 (m, 2H), 4.37 (m, 2H), 3.84 (s, 3H), 3.81 (s, 3H), 3.71 (s, 2H), 3.58 (s, 2H), 2.84 (t, J = 5.1 Hz, 2H), 2.77 (t, J = 4.7 Hz, 2H). ^{13}C NMR ($CDCl_3$) δ 157.7, 156.4, 156.2, 147.5, 147.1, 139.5, 137.0, 134.3, 134.2, 129.5, 129.0, 128.8, 128.7, 128.2, 128.1, 126.6, 126.2, 114.9, 111.4, 109.4, 74.0, 70.6, 65.5, 62.4, 55.90, 55.88, 55.7, 50.8, 28.7. MS CI (*i*-butane) *m/z* 594 $[M + H]^+$, mp = 101.8-102.7 °C (recrystallized from MeOH). Purity: 98%, t_r: 5.3 min., eluent: CH_3CN/H_2O 70/30 0.1% TFA, fl: 1.0 mL/min.

6,7-Dimethoxy-2-((4'-(3-((4-methoxy-1,2,5-oxadiazol-3-yl)oxy)ethoxy)biphen-4-yl)methyl)-1,2,3,4-tetrahydroisoquinoline (25). White solid. Yield 60% (CH_2Cl_2/EtOAc 80/20). ^{1}H NMR ($CDCl_3$) δ 7.54 (m, 4H), 7.45 (m, 2H), 7.01 (s, 1H), 6.98 (s, 1H), 6.61 (s, 1H), 6.50 (s, 1H), 4.71 (t, J = 4.5 Hz, 2H), 4.39 (t, J = 4.5 Hz, 2H), 4.10 (s, 3H), 3.84 (s, 3H), 3.81 (s, 3H), 3.72 (s, 2H), 3.58 (s, 2H), 2.85 (t, J = 5.1 Hz, 2H), 2.77 (t, J = 5.1 Hz, 2H). ^{13}C NMR ($CDCl_3$) δ 157.8, 157.0, 156.2, 147.5, 147.2, 139.5, 134.2, 130.3, 129.6, 128.6, 128.1, 127.1, 126.6, 114.9, 111.3, 109.4, 70.6, 65.5, 59.2, 56.1, 55.89, 55.88, 50.7, 29.7. MS CI (*i*-butane) *m/z* 518 $[M + H]^+$, mp = 123.4-124.0 °C (recrystallized from MeOH). Purity: 98%, t_r: 4.2 min., eluent: CH_3CN/H_2O 60/40 0.1% TFA, fl: 1.5 mL/min.

4-(2-((4'-((6,7-Dimethoxy-3,4-dihydroisoquinolin-2(1*H*)-yl)methyl)biphenyl-4-yl)oxy)ethoxy)-1,2,5-oxadiazol-3-carboxyamide (26). White solid. Yield 25% (CH_2Cl_2/EtOAc 50/50). ^{1}H NMR (DMSO-d_6) δ 8.30 (br s, 1H), 8.18 (br s, 1H), 7.61 (m, 4H), 7.41 (d, J = 8.2 Hz, 2H), 7.08 (d, J = 8.8 Hz, 2H), 6.66 (s, 1H), 6.59 (s, 1H), 4.72 (br s, 2H), 4.43 (br s, 2H), 3.70 (s, 3H), 3.66 (s, 3H), 3.45 (s, 2H), 2.73 (t, J = 3.8 Hz, 2H), 2.68 (t, J = 3.8 Hz, 2H). ^{13}C NMR (DMSO-d_6) δ 164.1, 158.5, 158.0, 148.0, 147.7, 143.1, 139.3, 137.9, 133.7, 130.2, 128.6, 127.4, 126.9, 126.6, 115.9, 112.6, 110.8, 72.4, 66.5, 62.5, 56.29, 56.28, 55.8, 51.5, 29.2. MS ESI+ *m/z* 531 $[M + H]^+$, mp = 208.4-209.0 °C (recrystallized from MeOH).

6,7-Dimethoxy-2-((4'-(3-((4-(phenylsulfinyl)-1,2,5-oxadiazol-3-yl)oxy)ethoxy)biphen-4-yl)methyl)-1,2,3,4-tetrahydroisoquinoline (27). Compound **23**, obtained by the general procedure reported above, was used without purification and was reacted following a reported procedure[25] to afford **27** in 20% overall yield as a white solid. ^{1}H NMR ($CDCl_3$) δ 7.77 (m, 2H), 7.51 (m, 9H), 6.92 (d, J = 9.0 Hz, 2H), 6.61 (s, 1H), 6.50 (s, 1H), 4.63 (t, J = 4.5 Hz, 2H), 4.23 (t, J = 4.5 Hz, 2H), 3.84 (s, 3H), 3.81 (s, 3H), 3.73 (s, 2H), 3.59 (s, 2H), 2.85 (t, J = 5.1 Hz, 2H),

2.78 (t, J = 5.1 Hz, 2H). ^{13}C NMR ($CDCl_3$) δ 162.1, 157.6, 150.8, 147.5, 147.2, 139.37, 139.35, 137.1, 134.3, 132.4, 129.6, 129.5, 128.2, 128.1, 126.6, 126.2, 125.0, 114.8, 111.4, 109.4, 71.3, 65.4, 62.4, 55.89, 55.88, 55.7, 50.8, 28.7. MS CI (*i*-butane) *m/z* 611 $[M + H]^+$, mp = 68.8-69.3 °C (trit. iPr_2O). Purity: 95%, t_r: 3.8 min., eluent: CH_3CN/H_2O 70/30 0.1% TFA, fl: 1.0 mL/min.

4-(2-((4'-((6,7-Dimethoxy-3,4-dihydroisoquinolin-2(1*H*)-yl)methyl)biphenyl-4-yl)oxy)ethoxy)-1,2,5-oxadiazol-3-carbonitrile (28). Compound **26** was solubilized in THF. The solution was cooled in an ice bath and Et_3N (4 eq) and TFAA (4 eq). were added. The mixture was stirred at room temperature overnight, after which solvent was removed under reduced pressure, the residue was taken up with CH_2Cl_2 and washed with 0.5 N NaOH, water (3 times) and brine. The organic layer was dried over Na_2SO_4, filtered and evaporated under reduced pressure. The crude product was purified by flash chromatography on silica gel, eluting with petroleum ether/EtOAc 55/45 to afford the title product as a pale-yellow sticky solid in 53% yield. ^{1}H NMR ($CDCl_3$) δ 7.55 (m, 4H), 7.48 (m, 2H), 7.0 (d, J = 8.2 Hz, 2H), 6.91 (s, 1H), 6.49 (s, 1H), 4.8, (t, J = 6.0 Hz, 2H), 4.42 (t, J = 6.0 Hz, 2H), 3.84 (s, 3H), 3.81 (s, 3H), 3.78 (s, 2H), 3.65 (s, 2H), 2.87 (br s, 4H). ^{13}C NMR ($CDCl_3$) δ 164.9, 164.7, 157.5, 151.2, 147.7, 147.3, 139.7, 134.4, 129.8, 128.2, 126.7, 125.7, 125.6, 114.9, 111.3, 109.4, 106.1, 72.3, 65.2, 61.8, 55.9 (two overlapping peaks), 55.1, 50.5, 28.1. MS ESI+ *m/z* 513 $[M + H]^+$. Purity: 98%, t_r: 4.4 min., eluent: CH_3CN/H_2O 60/40 0.1% TFA, fl: 1.2 mL/min.

4-((4'-((6,7-Dimethoxy-3,4-dihydroisoquinolin-2(1*H*)-yl)methyl)biphenyl-4-yl)oxy)butan-1-ol (29). To a solution of **1** in CH_3CN, 4-chlorobutan-1-ol (2 eq), Cs_2CO_3 (2 eq) and KI (0.10 eq) were added. The mixture was stirred at 70 °C for 96 hours. It was then diluted with CH_2Cl_2, washed with water, brine, dried over Na_2SO_4, filtered and evaporated under reduced pressure. The crude product was purified by flash chromatography on silica gel eluting with

CH_2Cl_2/MeOH 98/2 to afford the product as a colorless oil in 55% yield. ^{1}H NMR ($CDCl_3$) δ 7.52 (m, 4H), 7.44 (m, 2H), 6.96 (d, J = 8.4 Hz, 2H), 6.60 (s, 1H), 6.49 (s, 1H), 4.04, (t, J = 6.0 Hz, 2H), 3.84 (s, 3H), 3.80 (s, 3H), 3.72 (m, 4H), 3.85 (s, 2H), 2.83 (t, J = 5.1 Hz, 2H), 2.77 (t, J = 4.8 Hz, 2H), 1.90 (m, 2H), 1.77 (m, 2H). ^{13}C NMR ($CDCl_3$) δ 158.4, 147.5, 147.2, 139.6, 136.8, 133.5, 129.6, 128.0, 126.64, 126.56, 126.2, 114.8, 111.4, 109.5, 67.6, 62.5, 62.4, 55.89, 55.88, 55.7, 50.8, 29.5, 28.7, 25.8. MS CI (*i*-butane) *m/z* 448 $[M + H]^+$.

6,7-Dimethoxy-2-((4'-(3-((4-methoxy-1,2,5-oxadiazol-3-yl)oxy)butoxy)biphen-4-yl)methyl)-1,2,3,4-tetrahydroisoquinoline (30). White solid. Yield 73% (CH_2Cl_2/EtOAc 80/20). ^{1}H NMR ($CDCl_3$) δ 7.53 (m, 4H), 7.44 (d, J = 8.2 Hz, 2H), 6.95 (d, J = 8.8 Hz, 2H), 6.61 (s, 1H), 6.50 (s, 1H), 4.43, (t, J = 6.2 Hz, 2H), 4.06 (m, 5H), 3.84 (s, 3H), 3.81 (s, 3H), 3.71 (s, 2H), 3.58 (s, 2H), 2.84 (t, J = 5.1 Hz, 2H), 2.76 (t, J = 5.1 Hz, 2H), 2.03 (m, 4H). ^{13}C NMR ($CDCl_3$) δ 158.3, 157.1, 156.3, 147.5, 147.2, 139.6, 136.8, 133.6, 129.5, 128.0, 126.7, 126.6, 126.2, 114.7, 111.4, 109.4, 72.2, 67.2, 62.4, 59.1, 55.90, 55.88, 55.7, 50.8, 28.7, 25.7, 25.6. MS CI (*i*-butane) *m/z* 546 $[M + H]^+$, mp = 92.0-92.6 °C (recrystallized from *i*PrOH). Purity: 96%, t_r: 4.8 min., eluent: CH_3CN/H_2O 70/30 0.1% TFA, fl: 1.0 mL/min.

General procedure for the synthesis of furazan intermediates 6 – 9.

The appropriate alcohol (1.2 eq.) and 1,8-diazabicyclo[5.4.0]undec-7-ene (DBU, 3.5 eq.) were dissolved in CH_2Cl_2. 3,4-bisphenylsulfonylfurazan was added to the solution and the mixture was stirred at room temperature for 4 hours. The solution was then washed with water, brine, dried over Na_2SO_4, filtered and evaporated under reduced pressure. The residue was purified by flash chromatography (eluent: petroleum ether/CH_2Cl_2 60/40).

3-Phenoxy-4-(phenylsulfonyl)-1,2,5-oxadiazole (6). White solid. Yield 88%. ^{1}H NMR ($CDCl_3$) δ 8.16 (m, 2H), 7.79 (m, 1H), 7.66 (m, 2H), 7.43 (m, 2H), 7.29 (m, 3H). ^{13}C NMR ($CDCl_3$) δ 161.0, 153.8, 149.6, 137.8, 135.7, 130.0, 129.8, 129.1, 126.7, 119.2. MS CI (*i*-butane) *m/z* 303 $[M + H]^+$, mp = 97.7-98.4 °C (recrystallized from *i*PrOH).

3-(Benzyloxy)-4-(phenysulfonyl)-1,2,5-oxadiazole (7). White solid. Yield 93%. ^{1}H NMR ($CDCl_3$) δ 8.05 (d, J = 7.7 Hz, 2H), 7.73 (t, J = 7.3 Hz, 1H), 7.56 (t, J= 7.7 Hz, 2H), 7.39 (br s, 5H), 5.37 (s, 2H). ^{13}C NMR ($CDCl_3$) δ 161.1, 148.9, 137.8, 135.4, 133.6, 129.6, 129.2, 129.0, 128.8, 128.4, 75.1. MS CI (*i*-butane) *m/z* 317 $[M + H]^+$, mp = 91.2-91.9 °C (recrystallized from EtOH).

3-Methoxy-4-(phenylsulfonyl)-1,2,5-oxadiazole (9). White solid. Yield 67%. ^{1}H NMR ($CDCl_3$) δ 8.09 (d, J = 8.4 Hz, 2H), 7.77 (m, 1H), 7.64 (m, 2H), 4.16 (s, 3H). ^{13}C NMR ($CDCl_3$) δ 162.1, 148.7, 137.8, 135.5, 129.7, 128.9, 60.4. MS CI (*i*-butane) *m/z* 241 $[M + H]^+$, mp = 60.0-60.5 °C (recrystallized from EtOH).

3-Carbamoyl-4-(phenylsulfonyl)-1,2,5-oxadiazole (10). Compound **31** (1.86 mmol) was refluxed in 5 mL of trimethylphosphite for 18 hours. The mixture was then poured into cracked ice containing 2 mL of 37% HCl. After melting, the mixture was filtered under reduced pressure and a white solid was collected. Mother liquors were then extracted with EtOAc (3 times) and the extracts were washed with 1N HCl (3 times), $NaHCO_3$ saturated solution, and brine. The organic phase was dried over Na_2SO_4, filtered, and evaporated under reduced pressure. The white solid was unified with the filtration residue to afford the title product with 76% yield. ^{1}H NMR (DMSO-d_6) δ 8.71 (br s, 1H), 8.49 (br s, 1H), 8.13 (d, J = 7.7 Hz, 2H), 7.91 (t, J = 6.9 Hz,

1H), 7.77 (t, J = 7.4 Hz, 2H). ^{13}C NMR (DMSO-d_6) δ 157.05, 157.01, 149.1, 138.1, 136.9, 130.8, 129.8. MS ESI+ *m/z* 254 $[M + H]^+$, mp = 161.8-162.5 °C (recrystallized from MeOH).

Biology

Cell culture

MDCK-MDR1 and MDCK-MRP1 cells were a gift from Prof. P. Borst, NKI-AVL Institute, Amsterdam, The Nethererlands; Caco-2 cells were a kind gift from Dr. Aldo Cavallini and Dr. Caterina Messa of the Laboratory of Biochemistry, National Institute for Digestive Diseases, "S. de Bellis", Bari (Italy). MDCK cells and Caco-2 cells were grown in high glucose DMEM supplemented with 10% fetal bovine serum, 2mM glutamine,100 U/mL penicillin, 100 mg/mL streptomycin, in a humidified incubator at 37 °C with a 5% CO_2 atmosphere.

Calcein-AM experiment

These experiments were carried out as described elsewhere.[13] Each cell line, MDCK-MDR1 and MDCK-MRP1, (50,000 cells per well) was seeded into black CulturePlate 96/wells plate with 100 μL medium and allowed to become confluent overnight. 100 μL of test compounds were solubilized in culture medium and added to monolayers. A 96-wells plate was incubated at 37 °C for 30 min. Calcein-AM was added in 100 μL of Phosphate Buffered Saline (PBS) to yield a final concentration of 2.5 μM, and the plate was incubated for 30 min. Each well was washed 3 times with ice-cold PBS. Saline buffer was added to each well and the plate was read with Victor™ X3 (Perkin Elmer) at excitation and emission wavelengths of 485 nm and 535 nm, respectively. In these experimental conditions, calcein cell accumulation in the absence/presence of tested compounds was evaluated, and the fluorescence basal level was determined on

untreated cells. In treated wells the increase of fluorescence over the basal level was measured. EC_{50} values were determined by fitting the fluorescence increase percentage versus log[dose].

ATPlite assay

The MDCK-MDR1 cells were seeded in a 96-well microplate in 100 μL of complete medium at a density $2x10^4$ cells/well.[13] The plate was incubated O/N in a humidified atmosphere with 5% CO_2 at 37 °C. The medium was removed and 100 μL of complete medium, in the presence or absence of different concentrations of test compounds, were added. The plate was incubated for 2h in a humidified atmosphere with 5% CO_2 at 37 °C. 50 μL of mammalian cell lysis solution were added to each well, and the plate shaken for five minutes in an orbital shaker. 50 μL of substrate solution were added to each well and the plate shaken for five minutes in an orbital shaker. The plate was dark-adapted for ten minutes, and the luminescence measured.

Permeability Experiment. Preparation of Caco-2 Monolayer

Caco-2 cells were harvested with trypsin−EDTA, and seeded onto a MultiScreen Caco-2 assay system at a density of 10, 000 cells/well. The culture medium was replaced every 48 h for the first 6 days, and every 24 h thereafter; after 21 days in culture, the Caco-2 monolayer was utilized for permeability experiments. The transepithelial electrical resistance (TEER) of the monolayers was measured daily, before and after the experiment, using an epithelial voltohmmeter (Millicell-ERS; Millipore, Billerica, MA). The resulting TEER values are in most cases above 1000 Ω for a 21-day culture.[13]

Drug Transport Experiment

Apical to basolateral (P_{app} A→B) and basolateral to apical (P_{app} B→A) permeability of drugs was measured at 120 minutes at the concentration of 100 μM. Drugs were dissolved in Hank's balanced salt solution (HBSS, pH 7.4) and sterile filtered. After 21 days of cell growth, the medium was removed from filter wells and from receiver plate. The filter wells were filled with 75 μL of fresh HBSS buffer, and the receiver plate, with 250 μL per well of the same buffer. This procedure was repeated twice, and the plates were incubated at 37 °C for 30 min. After incubation, the HBSS buffer was removed, and, in some wells, drug solutions were added to the filter well (75 μL); drug-free HBSS without drug was added to the corresponding receiver plate (250 μL).

For other wells, the drug solutions were added to the apical (100 μL) or basolateral side (250 μL), and drug-free HBSS was added to the corresponding filter wells. The plates were incubated at 37 °C for 120 min. After incubation, samples were removed from both the apical (filter well) and the basolateral (receiver plate) sides of the monolayer, and analyzed. The concentration of compounds was determined using UV−vis spectroscopy. The apparent permeability (P_{app}), in nm/s units, was calculated using the following equation:

$$Papp = [VA/(area \times time)] \times ([drug]acceptor / [drug]initial)$$

where VA is the volume (in mL) in the acceptor well, *area* is the surface area of the membrane (0.11 cm^2 of the well), *time* is the total transport time in seconds (7200 s), [drug]acceptor is the concentration of the drug measured by UV spectroscopy, and [drug]initial is the initial drug concentration (1×10^{-4} M) in the apical or basolateral well.

Hoechst 33342 experiment

These experiments were carried out as described by Bauer et al. with modifications.[26] Each cell line (30,000 cells per well) was seeded into black CulturePlate 96/wells plate with 100 µl medium and allowed to become confluent overnight. 100 µl of test compounds were solubilized in culture medium and added to monolayers. 96/Wells plate was incubated at 37°C for 30 min. Hoechst 33342 was added in 100 µl of Phosphate Buffered Saline (PBS) to yield a final concentration of 8 µM and plate was incubated for 60 min. The supernatants were drained and the cells were fixed for 20 min under light protection using 100 µL per well of a 4% PFA solution. Each well was washed once with ice cold PBS. Saline buffer was added to each well and the plate was read to Victor3 (PerkinElmer) at excitation and emission wavelengths of 340/35 nm and 485/20 nm, respectively. In these experimental conditions Hoechst 33342 accumulation in the absence and in the presence of tested compounds was evaluated and fluorescence basal level was estimated by untreated cells. In treated wells the increase of fluorescence with respect to basal level was measured. EC_{50} values were determined by fitting the fluorescence increase percentage versus log[dose].

Antiproliferative assay

Determination of cell growth was performed using the MTT assay at 24 and 48 h. On day 1, 30000 cells/well were seeded into 96-well plates in a volume of 100 µL. On day 2, the various drugs concentration (0.1 µM-100 µM) were added. In all the experiments, the various drug-solvents (ethanol, DMSO) were added in each control to evaluate a possible solvent cytotoxicity. After the established incubation time with drugs, MTT (0.5 mg/mL) was added to each well, and after 3 h incubation at 37°C, the supernatant was removed. The formazan crystals were

solubilized using 100 µL of DMSO and the absorbance values at 570 and 630 nm were determined on the microplate reader Victor3 from PerkinElmer Life Sciences.

Analytical Methods

Samples from in-vitro permeability studies were analyzed using a Shimadzu spectrophotometer, UV-1800. For each compound, a calibration curve was constructed at the appropriate wavelength.

Molecular modeling

MODELLER 9.15[27] software was used for the comparative building of the human P-gp using the apo form of the mouse P-gp (PDB code 4Q9H). Starting from the sequence alignment with chain A of the reference template, 500 different conformational solutions were produced with the "refine_slow" routine; the best model was then selected using the DOPE (Discrete Optimized Protein Energy[28]) scoring function implemented in the software.

Ligand molecular scaffold in ionized form, with standard bond lengths and valence angles, were computed upon AM1 minimization, with the NDDO semi-empirical tool implemented in the Maestro software package.[29]

The molecular dynamic simulation of the solvated structures was performed using the Desmond system builder tool implemented in Maestro.[30] Dynamics were run on a NVDIA Quadro K4000 GPU at constant temperature (300 K) and pressure (1 bar) for a total of 240 ns, using default settings and the relaxation protocol of Desmond, with an energy and trajectory recording interval of 1.2 ps.

Dockings of **25** were initially carried out with VINA 1.1.2[31], submitting all the conformations of the molecular dynamics trajectory to rigid-body docking. The search space was selected by increasing its sizes by 30 Å in each of the three dimensions from the center of transmembrane domains, after which AUTODOCK 4.2[32] was used in a flexible docking.

Affinity maps were calculated on a 90×65×65 rectangular box, 0.375 Å spaced, centered on the best VINA pose. The population size and the number of energy evaluations were set to 300 and 50000000, respectively. The puckering of the tetrahydroisoquinoline ring was not altered, according to the X-ray of **1**.[33] For the target structure, electrostatic charges were calculated according to the AMBER UNITED force field,[34] while AM1 implemented in the MacroModel software package[29] was applied to the ligand. All poses were then clustered to a value of RMSD = 2 Å, and ranked according to the relative Free Energy of Binding (FEB).

The best VINA pose was taken as a template for a shape-based superposition of compounds **15**, **17** and **30**, achieved by means of the ROCS algorithm (ROCS 3.2.0.4: OpenEye Scientific Software, Santa Fe, NM).[35] For each ligand, 2000 conformers were generated with OMEGA (OMEGA 2.5.1.4: OpenEye Scientific Software, Santa Fe, NM),[36] and the shape objective function was used to rank the ligand database and select the best molecular overlay, i.e. that with the highest Tanimoto coefficient. In order to save computational time, and due to the extreme flexibility of the ligands data set, docking was then pursued with the lone local minimization procedure, and assigning flexibility to the side chains of His61, Leu65, Gln195, Tyr310, Gln946, Met949 and Tyr950.

AUTHOR INFORMATION

Corresponding Authors

*S.G. e-mail: stefano.guglielmo@unito.it. Phone: (+39)116707678. *N.A.C. e-mail: nicolaantonio.colabufo@uniba.it . Phone (+39)805442727.

Notes

The authors declare no competing financial interest.

ACKNOWLEDGMENT

This study was supported by University of Turin, grant „Ricerca Locale–GUGSRILO13“.

ABBREVIATIONS

ABC, ATP binding cassette; AM1, Austin model 1; BCRP, breast cancer resistance protein; Caco-2, colorectal adenocarcinoma cells; DBU, 1,8-diazabicyclo[5.4.0]undec-7-ene; DMEM, Dulbecco's modified eagle medium; DMF, dimethylformamide; DOPE, discrete optimized protein energy; EDTA, ethylenediaminetetraacetic acid; FEB, free energy of binding; HBSS, Hank's balanced salt solution; MDCK, Madin-Darby canine kidney; MDR, multidrug resistance; MRP1, multidrug resistance-associated protein; NDDO, neglect of diatomic differential overlap; P_{app}, apparent permeability; PBS, phosphate buffered saline; PET, positron emission tomography; P-gp, P-glycoprotein; RMSD, root mean square deviation; RP-HPLC, reversed phase high performance liquid chromatography; SPECT, single photon emission computed tomography; TEER, transepithelial electrical resistance; TFAA, trifluoroacetic anhydride; THF, tetrahydrofuran; TLC, thin layer chromatography.

References

(1) Colabufo, N. A.; Berardi, F.; Cantore, M.; Perrone, M.G.; Contino, M.; Inglese, C.; Niso, M.; Perrone, R.; Azzariti, A.; Simone, G. M.; Paradiso, A. 4-Biphenyl and 2-naphthyl substituted 6,7-dimethoxytetrahydroisoquinoline derivatives as potent P-gp modulators. *Bioorg. Med. Chem.* **2008**, *16*, 3732-3743.

(2) Colabufo, N. A.; Berardi, F.; Cantore, M.; Contino, M.; Inglese, C.; Niso, M.; Perrone, R. Perspectives of P-glycoprotein modulating agents in oncology and neurodegenerative diseases: pharmaceutical, biological and diagnostic potentials. *J. Med. Chem.* **2010**, *53*, 1883-1897.

(3) Colabufo, N. A.; Berardi, F.; Contino, M.; Niso, M.; Perrone, R. ABC pumps and their role in active drug transport. Special Issue, *Curr. Topics Med. Chem.* **2009**, *9*, 119-129.

(4) Planting, A. S.; Sonneveld, P.; van der Gaast, A.; Sparreboom, A.; van der Burg, M. E.; Luyten, G. P.; de Leeuw, K.; de Boer-Dennert, M.; Wissel, P. S.; Jewell, R. C.; Paul, E. M.; Purvis, N. B. Jr.; Verweij, J. A phase I and pharmacologic study of the MDR converter GF120918 in combination with doxorubicin in patients with advanced solid tumors. *Cancer Chemother. Pharmacol.* **2005**, *55*, 91–99.

(5) Kuppens, I. E.; Witteveen, E. O.; Jewell, R. C.; Radema, S. A.; Paul, E. M.; Mangum, S. G.; Beijnen, J. H.; Voest, E. E.; Schellens, J. H. A phase I, randomized, open-label, parallel-cohort, dose finding study of elacridar (GF120918) and oral topotecan in cancer patients. *Clin. Cancer Res.* **2007**, *13*, 3276–3285.

(6) Fox, E.; Bates, S. E. Tariquidar (XR9576): a P-glycoprotein drug efflux pump inhibitor. *ExpertRev. Anticancer Ther.* **2007**, *7*, 447–459.

(7) Pusztai, L.; Wagner, P.; Ibrahim, N.; Rivera, E.; Theriault, R.; Booser, D.; Symmans, F. W.; Wong, F.; Blumenschein, G.; Fleming, D. R.; Rouzier, R.; Boniface, G.; Hortobagyi, G. N. Phase II study of tariquidar, a selective P-glycoprotein inhibitor, in patients with chemotherapy-resistant, advanced breast carcinoma. *Cancer* **2005**, *104*, 682–691.

(8) Riganti, C.; Miraglia, E.; Viarisio, D.; Costamagna, C.; Pescarmona, G.; Ghigo, D.; Bosia, A. Nitric oxide reverts the resistance to doxorubicin in human colon cancer cells by inhibiting the drug efflux. *Cancer Res.* **2005**, *65*, 516–525.

(9) Fruttero, R.; Crosetti, M.; Chegaev, K.; Guglielmo, S.; Gasco, A.; Berardi, F.; Niso, M.; Perrone, R.; Panaro, M. A.; Colabufo, N. A. Phenylsulfonylfuroxans as modulators of multidrug-resistance-associated protein-1 and P-glycoprotein. *J. Med. Chem*. **2010**, *53*, 5467-5475.

(10) Chegaev, K.; Riganti, C.; Lazzarato, L.; Rolando, B.; Guglielmo, S.; Campia, I.; Fruttero, R.; Bosia, A.; Gasco, A. Nitric oxide donor doxorubicins accumulate into doxorubicin-resistant human colon cancer cells inducing cytotoxicity. *ACS Med. Chem. Lett.* **2011**, I, 494-497.

(11) Riganti, C.; Rolando, B.; Kopecka, J.; Campia, I.; Chegaev, K.; Lazzarato, L.; Federico, A.; Fruttero, R.; Ghigo, D. Mitochondrial-targeting nitrooxy-doxorubicin: a new approach to overcome drug resistance. *Mol. Pharm.* **2013**, *10*, 161-174.

(12) a. Löscher, W.; Potschka, H. Role of drug efflux transporters in the brain for drug disposition and treatment of brain diseases. *Prog. Neurobiol.* **2005**, *76*, 22-76. b. Abuznait, A. H.; Kaddoumi, A. Role of ABC transporters in the pathogenesis of Alzheimer's disease. *ACS Chem. Neurosci.* **2012**, *3*, 820−831.

(13) Capparelli, E.; Zinzi, L.; Cantore, M.; Contino, M.; Perrone, M. G.; Luurtsema, G.; Berardi, F.; Perrone, R.; Colabufo, N. A. SAR studies on tetrahydroisoquinoline derivatives: the role of flexibility and bioisosterism to raise potency and selectivity on P-gp protein. *J. Med. Chem.* **2014,** *57*, 9983-9994.

(14) Guglielmo, S.; Contino, M.; Lazzarato, L.; Perrone, M. G.; Blangetti, M.; Fruttero, R.; Colabufo, N. A. A potent and selective P-gp modulator for altering Multidrug Resistance due to pump overexpression. *ChemMedChem*. **2016**, *11*, 374-376.

(15) Colabufo, N. A.; Fruttero, R.; Guglielmo, S. Unpublished results.

(16) Szewczyk, P.; Tao, H.; McGrath, A. P.; Villaluz, M.; Rees, S. D.; Lee, S. C.; Doshi, R.; Urbatsch, I. L.; Zhang, Q.; Chang, G. Snapshots of ligand entry, malleable binding and induced helical movement in P-glycoprotein. *Acta Crystallogr. D Biol. Crystallogr.* **2015**, *71*, 732-741.

(17) Ward, A. B.; Szewczyk, P.; Grimard, V.; Lee, C. W.; Martinez, L.; Doshi, R.; Caya, A.; Villaluz, M.; Pardon, E.; Cregger, C.; Swartz, D. J.; Falson, P. G.; Urbatsch, I. L.; Govaerts, C.; Steyaert, J.; Chang, G. Structures of P-glycoprotein reveal its conformational flexibility and an epitope on the nucleotide-binding domain. *Proc. Natl. Acad. Sci. USA*. **2013**, *110*, 13386-13391.

(18) Aller, S. G.; Yu, J.; Ward, A.; Weng, Y.; Chittaboina, S.; Zhuo, R.; Harrell, P. M.; Trinh, Y. T.; Zhang, Q.; Urbatsch, I. L.; Chang, G. Structure of P-glycoprotein reveals a molecular basis for poly-specific drug binding. *Science* **2009**, *323*, 1718-1722.

(19) Morris, G. M.; Huey, R.; Lindstrom, W.; Sanner, M. F.; Belew, R. K.; Goodsell, D. S.; Olson, A. J. AutoDock4 and AutoDockTools4: automated docking with selective receptor flexibility. *J. Comput. Chem.* **2009**, *16*, 2785-2791.

(20) Godford, P. J. A computational procedure for determining energetically favorable binding sites on biologically important macromolecules. *J. Med. Chem.* **1985**, *28*, 849-857.

(21) Boschi, D.; Di Stilo, A.; Cena, C.; Lolli, M. L.; Fruttero, R.; Gasco, A. Studies on agents with mixed NO-dependent vasodilating and β-blocking activities. *Pharm. Res.* **1997**, *14*, 1750-1758.

(22) Tosco, P.; Bertinaria, M.; Di Stilo, A.; Marini, E.; Rolando, B.; Sorba, G.; Fruttero, R.; Gasco, A. A new class of NO-donor H_3-antagonists. *Farmaco* **2004**, *59*, 359-371.

(23) Calvino, R.; Mortarini, V.; Gasco, A.; Sanfilippo, A.; Ricciardi, M. L. Antimicrobial properties of some furazan and furoxan derivatives. *Eur. J. Med. Chem.* **1980**, *15*, 485-487.

(24) Calvino, R.; Fruttero, R.; Ghigo, D.; Bosia, A.; Pescarmona, G. P.; Gasco, A. 4-Methyl-3-(arylsulfonyl)furoxans: a new class of potent inhibitors of platelet aggregation. *J. Med. Chem.* **1992**, *35*, 3296-3300.

(25) Venier, C. G.; Squires, T. G.; Chen, Y. Y.; Smith, B. F.. Peroxytrifluoroacetic acid oxidation of sulfides to sulfoxides and sulfones. *J. Org. Chem.* **1982**, *47*, 3773–3774.

(26) Capparelli, E.; Zinzi, L.; Cantore, M.; Contino, M.; Perrone, M. G.; Luurtsema, G.; Berardi, F.; Perrone, R.; Colabufo, N. A. SAR studies on tetrahydroisoquinoline derivatives: the role of flexibility and bioisosterism to raise potency and selectivity on P-gp protein. *J. Med. Chem.* **2014**, *57*, 9983-9994.

(27) Sali, A.; Blundell, T. L. Comparative protein modelling by satisfaction of spatial restraints. *J. mol. Biol.* **1993**, *234*, 779-815.

(28) Shen, M. Y.; Sali, A. Statistical potential for assessment and prediction of protein structures. *Protein Sci.* **2006**, *15*, 2507-2524.

(29) Schrödinger Release 2015-3: Maestro, version 10.3, Schrödinger, LLC, New York, NY, 2015.

(30) Bowers, K. J.; Chow, E.; Xu, H.; Dror, R. O.; Eastwood, M. P.; Gregersen, B. A.; Klepeis, J. L.; Kolossvary, I.; Moraes, M. A.; Sacerdoti, F. D.; Salmon, J. K.; Shan, Y.; Shaw, D. E. Scalable algorithms for molecular dynamics simulations on commodity clusters, Proceedings of the ACM/IEEE Conference on Supercomputing (SC06), Tampa, Florida, 2006, November 11-17 Schrödinger Release 2015-3: Desmond Molecular Dynamics System, version 4.3, D. E. Shaw Research, New York, NY, 2015. Maestro-Desmond Interoperability Tools, version 4.3, Schrödinger, New York, NY, 2015.

(31) Trott, O.; Olson, A. J. AutoDock Vina: improving the speed and accuracy of docking with a new scoring function, efficient optimization and multithreading. *J. Comp. Chem.* **2010**, *31*, 455-461.

(32) Morris, G. M.; Goodsell, D. S.; Halliday, R. S.; Huey, R.; Hart, W. E.; Belew, R. K.; Olson, A. J. Automated docking using a lamarckian genetic algorithm and empirical binding free energy function. *J. Comput. Chem.* **1998**, *19*, 1639-1662.

(33) Altomare, A.; Capparelli, E.; Carrieri, A.; Colabufo, N. A.; Moliterni, A.; Rizzi, R.; Siliqi, D. Crystallographic study of PET radio-tracers in clinical evaluation for early diagnosis of Alzheimers. *Acta Crystallogr. Sect. E Struct. Rep. Online.* **2014**, *70*, 1149-1150.

(34) Cornell, W. D.; Cieplak, P.; Bayly, C. I.; Gould, I. R.; Merz, K. M.; Ferguson, D. M.; Spellmeyer, D. C.; Fox, T.; Caldwell, J. W.; Kollman, P. A. A second generation force field for the simulation of proteins, nucleic acids, and organic molecules. *J. Am. Chem. Soc.* **1995**, *117*, 5179-5193.

(35) Hawkins, P. C. D.; Skillman, A. G.; Nicholls, A. Comparison of shape-matching and docking as virtual screening tools. *J. Med. Chem.* **2007**, *50*, 74-82.

(36) Hawkins, P. C. D.; Skillman, A. G.; Warren, G. L.; Ellingson, B. A.; Stahl, M. T. Conformer generation with OMEGA: algorithm and validation using high quality structures from the protein databank and Cambridge structural database. *J. Chem. Inf. Model.* **2010**, *50*, 572-584.

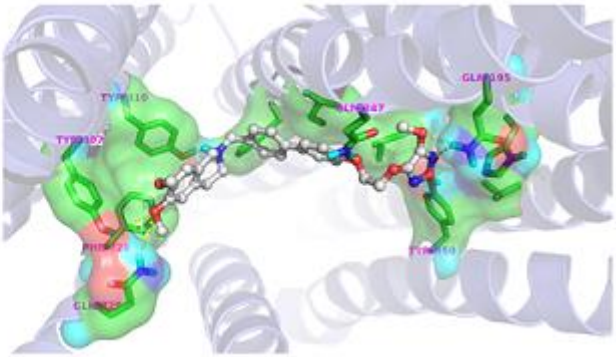

For table of contents only